

# HIGHLY ACCELERATED DIAMAGNETIC PLASMOIDS: A NEW X-RAY PRODUCTION MECHANISM FOR OB STELLAR WINDS

WAYNE L. WALDRON<sup>1</sup> AND JOSEPH P. CASSINELLI<sup>2</sup>  
*Accepted for publication in The Astrophysical Journal Letters*

## ABSTRACT

The observed X-ray source temperature distributions in OB stellar winds, as determined from high energy resolution *Chandra* observations, show that the highest temperatures occur near the star, and then steadily decrease outward through the wind. To explain this unexpected behavior, we propose a shock model concept that utilizes a well-known magnetic propulsion mechanism; *the surface ejection of “diamagnetic plasmoids” into a diverging external magnetic field*. This produces rapidly accelerating self-contained structures that plow through an ambient wind and form bow shocks that generate a range in X-ray temperatures determined by the plasmoid-wind relative velocities. The model free parameters are the plasmoid initial Alfvén speed, the initial plasma- $\beta$  of the external medium, and the divergence rate of the external field. These are determined by fitting the predicted bow shock temperatures with the observed OB supergiant X-ray temperature distribution. We find that the initial external plasma- $\beta$  has a range between 0 and 2, and the assumed radially-decreasing external magnetic field strength that scales as  $r^{-S}$  has a value of  $S$  lying between 2 and 3. Most importantly, the initial plasmoid Alfvén speed is found to be well-constrained at a value of  $0.6 V_\infty$ , which appears to represent an upper limit for all normal OB stars. This intriguing new limit on OB magnetic properties, as derived from *Chandra* observations, emphasizes the need for further studies of magnetic propulsion mechanisms in these stars.

*Subject headings:* shock waves – stars: early-type – stars: magnetic fields – stars: winds, outflows – X-rays: stars – X-rays: general

## 1. INTRODUCTION

Waldron & Cassinelli (2007, 2008; hereafter, WC07 and WC08) presented a detailed study of the *Chandra* HETGS data from 17 early-type stars (hereafter, OB stars). One of the more surprising results is the evidence for a radially dependent X-ray temperature ( $T_X$ ) distribution that steadily decreases outward through the stellar wind from a high value near the star. We suggest that this distribution may be related to stellar magnetic field effects, and present a semi-empirical model for X-ray production in OB stars that incorporates a well known magnetic ejection process.

The plausibility of magnetic ejection is supported by the increasing number of magnetic field detections on OB stars. There are now direct measurements of magnetic fields for three O-stars (Donati et al. 2002, 2006a; Bouret et al. 2008) and five early B-stars (Donati et al. 2001, 2006b; Neiner et al. 2003; Petit et al. 2008). The recent observation by Bouret et al. (2008) provides the first detection of a magnetic field on an O supergiant,  $\zeta$  Ori A (O9.7 Ib), with a field strength of 60 - 100 G. It also has a complex magnetic topology apparently similar to the magnetic field structure of  $\tau$  Sco (B0 V) that is interspersed with “hole regions” that may resemble the magnetospheric structure of the Sun (Donati et al. 2006b). This  $\zeta$  Ori A detection is of particular interest to us since magnetic field strengths similar to the observed value were proposed to explain its high energy X-ray emission lines in *Einstein* SSS data (Cassinelli &

Swank 1983) and *Chandra* HETGS data (Waldron & Cassinelli 2001).

Theoretical studies of magnetic fields in OB stars have primarily focused on studying origins; dynamo processes (Charbonneau & MacGregor 2001; MacGregor & Cassinelli 2003; Mullan & MacDonald 2005), and remnant fossil fields (Ferrario & Wickramasinghe 2005, 2006). In addition, Maeder et al. (2008) has shown that rapid rotation can extend the thickness of the thin outer convection zones in OB stars (Maeder 1980). At this early stage of studying OB surface magnetic field structures we can only surmise that these field structures may likely be analogous to solar emerging magnetic field regions (Zwaan 1985). Unlike recent research in solar physics our intent is not to explore ways of producing coronal regions around these stars, but rather to explain the observationally derived X-ray temperatures of hot shock fragments that are dispersed throughout their stellar winds.

## 2. THE $T_X$ DISTRIBUTION IN OB STARS

At the core of our semi-empirical model is the observed radial decreasing source  $T_X$  distribution found by WC07 (and updated in WC08) which is most noticeable for OB supergiants (see Fig. 1). This distribution is unexpected based on wind shock theory developed prior to the launch of *Chandra* (e.g., Feldmeier 1995). To analyze the significance of this  $T_X$  distribution we first obtain an empirical power-law fit (error-weighted) to the WC08 data (neglecting the  $\delta$  Ori A Ne IX data for reasons discussed by WC07) given by

$$T_X(r) = (18 \pm 2) \left( \frac{R_*}{r} \right)^{0.79 \pm 0.05} MK \quad (1)$$

<sup>1</sup> Eureka Scientific, Inc., 2452 Delmer St., Oakland CA, 94602; wwaldron@satx.rr.com

<sup>2</sup> Dept. of Astronomy, University of Wisconsin-Madison, Madison, WI 53711; cassinelli@astro.wisc.edu

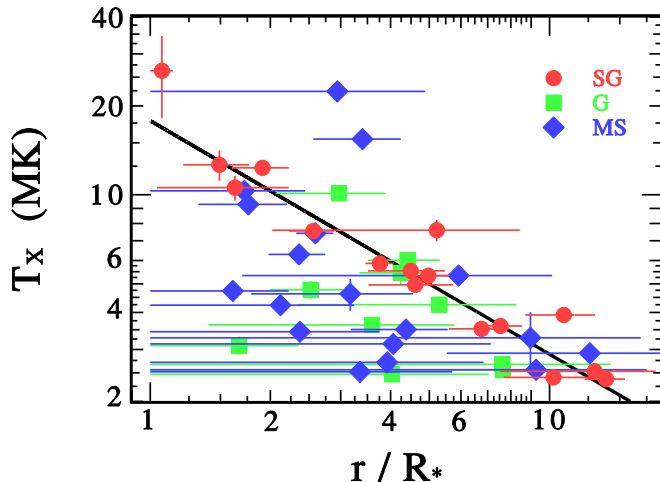


FIG. 1.— Comparison of the OB supergiant power-law fit given by Eq. (1) (black line) with the observed  $T_X$  for all OB supergiants (SG), giants (G), and main sequence (MS) stars as determined by WC08. The two data points significantly outside this bound are associated with the peculiar MS star  $\theta^1$  Ori C which has a very strong magnetic field of  $\approx 1000$  Gauss (Donati et al. 2002).

This power-law fit shows that very high  $T_X$  are present near the star and we think this expression will be useful for interpretations of the emission line results and for general modeling efforts. As shown in Figure 1, the lower luminosity class OB stars have more complex  $T_X$  distributions since these stars have winds that are more optically thin to X-rays, and there can be radially extended emission regions associated with any  $T_X$  value. Nevertheless, Figure 1 shows that nearly all giant and main sequence stars have an upper bound on  $T_X$ , and this upper bound is consistent with the supergiant power-law fit (Eq. 1). As discussed by WC07, clarifications of these observed  $T_X$  distributions should lead to a better understanding of the overall X-ray emission process in OB stars, and in § 3 we present a model that provides a viable explanation of this radially-dependent  $T_X$  upper bound.

### 3. PLASMOID MODEL

The primary goal of this paper is to find a process that can generate high X-ray temperatures at small stellar radii ( $\leq 1.5 R_*$ ). In the wind-clump model of Howk et al. (2000) they realized a need for high  $T_X$  at small radii and chose to consider the possibility of in-fall. Here we consider an alternative method of producing large relative velocities at small radii by using an early magnetic propulsion model suggested by Cargill & Pneuman (1984; hereafter CP84). They derived, in a straightforward way, the dynamics of isolated “diamagnetic plasmoids” that are launched into a diverging external magnetic field. The plasmoids are produced by magnetic reconnection events and are rapidly accelerated owing to the interaction of the plasmoid magnetic moment with the external field (Schluter 1957; Parker 1957; Pneuman 1983). We picture these plasmoids as being produced just above the photosphere, and due to the rapid acceleration, plow through the overlying stellar wind that has drawn out the external magnetic field. The plasmoid-wind interactions produce “bow shock” structures around the plas-

moids that are likely to be similar to those described by Cassinelli et al. (2008; hereafter CAS08), and the  $T_X$  will depend on the relative velocities between these plasmoids and the wind. An advantage of bow shock produced X-ray emission is that the emission measure is determined by the influx of the ambient wind material.

We neglect the effects of the line radiation force on these plasmoids because Abbott (1982) found that the line driving is dominated by those spectral lines that have energies slightly larger than the energy associated with the peak of the radiation field. Hence, for a parcel of gas that is in a higher stage of ionization than expected from the radiation temperature, the line force will be greatly reduced. The gas temperature of the plasmoid is likely to be higher than the surroundings because the magnetic reconnection process should generate sufficient energy to increase the temperature ionization state of the plasmoid (e.g., a gas temperature  $> 0.2$  MK should be sufficient to shift the dominant ions beyond the radiation field peak of OB stars). The plasmoid is expected to remain hot since it will heat up as it accelerates as shown by CP84. In addition, the X-rays from the bow shock formed on the outer plasmoid surface will also contribute to maintaining the higher level of ionization by the Auger effect as discussed CAS08.

The temperature of the X-ray source behind a shock depends on the relative velocity of the incident material and the shock front. Consequently, to produce the high  $T_X$  at low radii ( $< 1.5 R_*$ ) where the ambient wind velocity is low, these plasmoids must experience very rapid accelerations to generate the required large relative velocities. As shown by CP84, the largest accelerations can be achieved only for the case when the initial plasma- $\beta$  of the plasmoid,  $\beta_{po}$ , is  $\ll 1$ , where  $\beta_{po} = 8\pi P_p(r_o)/B_p(r_o)^2$  is the ratio of the initial plasmoid gas pressure to the initial magnetic pressure at the radius ( $r_o$ ) where the plasmoid is created. Using the momentum equation and the basic assumptions given by CP84, along with this condition on  $\beta_{po}$ , one can obtain an analytic expression for the plasmoid velocity (assuming the plasmoid velocity = 0 at  $r_o$ ),

$$V_P(r)^2 = 4V_{Apo}^2 \left( 1 - \gamma(r) \left( \frac{r_o}{r} \right)^{S/2} \right) - V_{es}^2 \left( 1 - \frac{r_o}{r} \right) \quad (2)$$

where  $V_{Apo} = B_p(r_o)/(4\pi\rho_p(r_o))^{1/2}$  is the initial plasmoid Alfvén speed,  $\rho_p(r_o) =$  initial plasmoid mass density,  $V_{es}$  is the stellar effective escape speed, and  $S$  is the exponent of the assumed radially-dependent external magnetic field,  $B_e(r) = B_e(r_o) (r_o/r)^S$ .

Equation (2) is more general than the one given by CP84 due to the presence of  $\gamma(r)$  which arise from the external gas pressure gradient contribution to the plasmoid acceleration. By allowing for a non-zero  $\beta_{eo}$  we derived equation (2) by starting with CP84 equation (2.16), and found that  $\gamma(r)$  is

$$\gamma(r) = \left( \frac{1 + \beta_e(r)}{1 + \beta_{eo}} \right)^{1/4} \quad (3)$$

where  $\beta_e(r) = 8\pi P_e(r)/B_e(r)^2$  is the radially-dependent external plasma- $\beta$ , and  $\beta_{eo} = \beta_e(r_o)$ . In the limit of  $\beta_e(r) \rightarrow 0$  (i.e.,  $\beta_{eo} \rightarrow 0$  and  $\gamma \rightarrow 1$ ), equation (2) re-

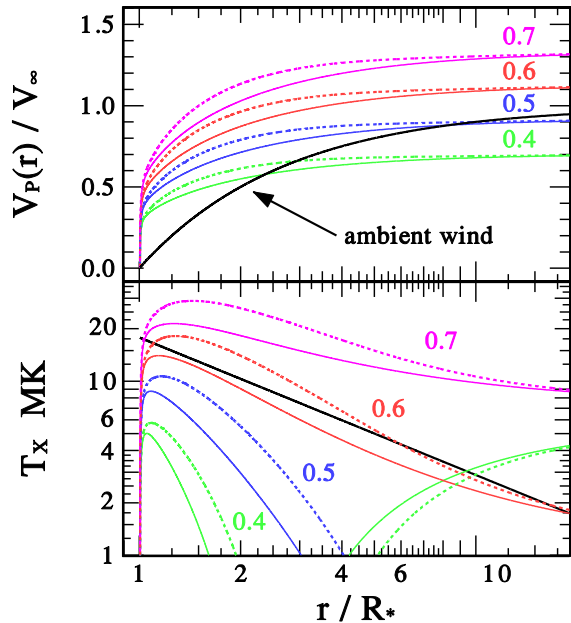


FIG. 2.— Parameter study of the plasmoid model  $V_P$  (top panel) and  $T_X$  (bottom panel) dependence on  $V_{Apo}/V_\infty = 0.4, 0.5, 0.6, 0.7$  for a fixed value of  $\beta_{eo} = 1$ . For each  $V_{Apo}/V_\infty$ , two curves are presented, for  $S = 2$  (solid line) and  $S = 3$  (dashed line). In top panel, the ambient wind velocity law is shown as a solid black line. In bottom panel, the solid black line represents the power-law fit given by Eq. (1).

duces to equation (3.2) of CP84. In this initial study we assume that the external temperature is isothermal and equal to the stellar effective temperature and the overlying wind is spherical symmetric which are common assumptions used in the development of basic wind models (e.g., Lamers & Cassinelli 1999). Hence, for  $\beta_e(r) > 0$ ,  $\gamma(r)$  will be  $< 1$  and the plasmoid will experience an enhanced acceleration as discussed below (see Fig. 3).

Although bow shock structures generate a range of  $T_X$  around a plasmoid at any given radius (see CAS08), in this paper we are only concerned with the maximum  $T_X$  that occurs at the apex of the bow shock. From the Rankine-Hugoniot temperature relation, this maximum bow shock  $T_X(r)$  is

$$T_X(r) = 14 \left( \frac{\Delta V(r)}{1000} \right)^2 \text{ MK} \quad (4)$$

where  $\Delta V(r) = V_P(r) - V_W(r)$  (measured in  $\text{km s}^{-1}$ ) is the maximum (apex) relative velocity between the plasmoid and the wind. For the ambient wind velocity ( $V_W$ ) we adopt the commonly used expression,  $V_W(r) = V_\infty(1 - R_*/r)$ . For  $\Delta V > 0$ , the plasmoid is moving faster than the ambient wind and the bow shock is formed on the outward-facing side of the plasmoid. Conversely, for  $\Delta V < 0$ , the bow shock is formed on the star-ward side of the plasmoid since it is moving slower than the wind, a condition more likely at large wind radii.

We present a series of models to illustrate the dependence of  $T_X$  on the three basic parameters ( $V_{Apo}$ ,  $\beta_{eo}$ ,

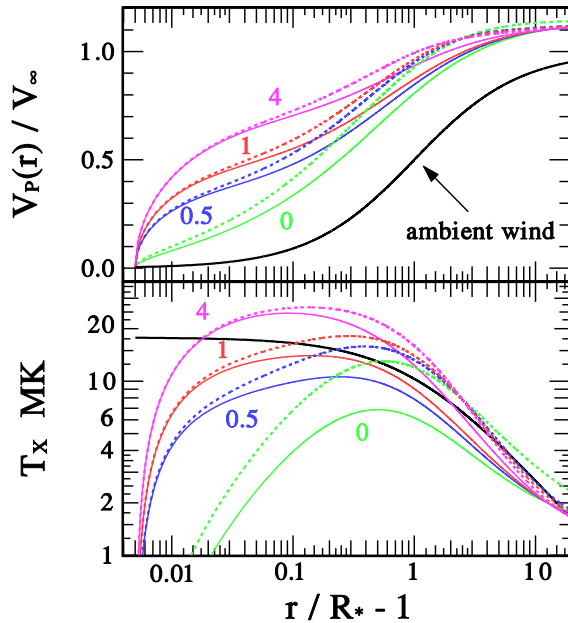


FIG. 3.— Same as Figure 2 but for the parameter study of  $\beta_{eo} = 0, 0.5, 1, 4$ , using a fixed value of  $V_{Apo}/V_\infty = 0.6$ . The radius axis has been re-scaled to magnify the details at small radii where  $\beta_{eo}$  effects are most prominent.

$S$ ). We use a  $V_\infty = 2158 \text{ km s}^{-1}$  and a  $V_{es} = 782 \text{ km s}^{-1}$  which represent averages of the OB supergiants with measured  $T_X$  values. We set  $r_o = 1.005 R_*$  which corresponds to an initial ambient wind velocity of  $\sim 1/2$  times the thermal speed using a mean effective temperature of 36,000 K. The functional radial dependencies of  $T_X$  on  $V_{Apo}/V_\infty$ ,  $\beta_{eo}$ , and  $S$  are shown in Figures 2 and 3. As is evident in Figure 2, the ratio  $V_{Apo}/V_\infty$  is the dominant parameter determining the overall magnitude of the observed  $T_X$  distribution. Figure 3 shows that large changes in  $\beta_{eo}$  are required to affect the  $T_X$  distribution, but only below  $2 R_*$ . An increase in  $\beta_{eo}$  produces a rise in the peak  $T_X$  and shifts it to smaller radii. The field divergence parameter,  $S$ , primarily produces small vertical shifts in the  $T_X$  distribution.

Non-linear least-squared fit models (A & B) are obtained by fitting the model  $T_X$  (Eq. 4) to the observed OB supergiant  $T_X$  distribution using the supergiant  $V_\infty$  and  $V_{es}$  averages. The model fits are shown in Figure 4 and best-fit parameters are listed in Table 1. Model A uses all the data, and Model B neglects the very high  $T_X$  ( $\approx 26 \text{ MK}$ ) at  $\approx 1.1 R_*$  that is associated with Cyg OB2 No. 8a. As evident in our parameter study, both models predict a well-constrained value for  $V_{Apo}/V_\infty$ , emphasizing the importance of this parameter in explaining the  $T_X$  distribution. As for the other two parameters, the constraints are less stringent as shown in Table 1. The high  $\beta_{eo}$  is necessary to fit the Cyg OB2 No. 8a low radius, high  $T_X$  value, as demonstrated in our  $\beta_{eo}$  parameter study shown in Figure 3. As shown in Figure 4, the two model fits (A and B) are essentially identical above  $2 R_*$ , whereas, below  $2 R_*$ , the models are more sensitivity to the values of  $\beta_{eo}$  and

TABLE 1  
PLASMOID MODEL BEST-FIT PARAMETERS

Model	$V_{Apo}/V_{\infty}$	$\beta_{eo}$	$S$	$\chi^2/DOF$
Model A	$0.61 \pm 0.01$	$1.3 \pm 0.9$	$2.2 \pm 0.3$	17/13
Model B	$0.60 \pm 0.01$	$0.28 \pm 0.31$	$2.6 \pm 0.2$	15/12

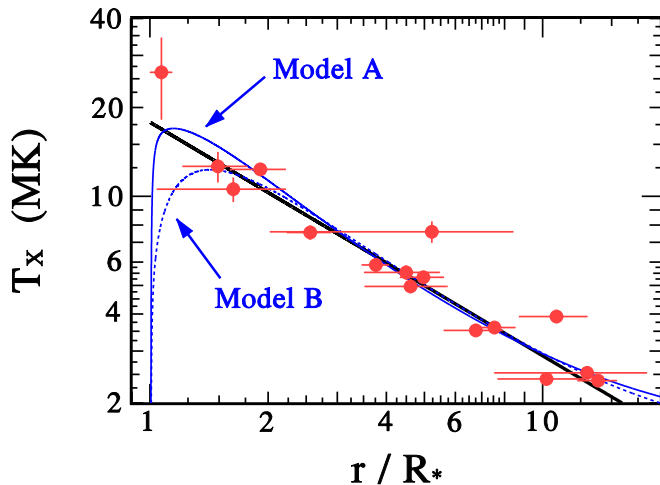


FIG. 4.— Comparison of the two plasmoid ejection model fits to the observed  $T_X$  distribution of OB supergiants; Model A (solid blue line) and Model B (dashed blue line). See Table 1 and discussion in §3. The solid black line represents the power-law fit given by Eq. (1).

$S$ .

From the derived value of  $V_{Apo} = 0.60 V_{\infty}$  we can check the assumption that  $\beta_{po} \ll 1$ , which is fundamental to the validity of equation (2), and we also derive a plasmoid initial density. By writing  $\beta_{po} = 2(a_p/V_{Apo})^2 = 0.02 T_6$ , where  $a_p$  is the plasmoid initial thermal speed ( $T_6$  has units of MK), a value of  $\beta_{po} < 0.1$  requires a  $T_6 < 5$ . To satisfy the requirement for an enhanced ionization state in the plasmoid as discussed earlier, all that is needed is a plasmoid temperature  $> 0.2$  MK, well below this upper limit. Assuming that the detected field of  $\approx 80$  G from  $\zeta$  Ori A is typical for the initial external field in all OB supergiants, we estimate from  $V_{Apo}$  an OB supergiant plasmoid initial density of  $4 \times 10^{10}(1 + \beta_{eo}) \text{ cm}^{-3}$

where we have used the total pressure balance equation,  $B_p(r_o)^2 = B_e(r_o)^2(1 + \beta_{eo})$ . Since this density is much lower than that expected for the surrounding external gas close to the star, these plasmoids should not be visualized as clumps, but more appropriately, as isolated magnetic rarefactions.

#### 4. DISCUSSION

We have presented a novel idea that can explain the near-surface high X-ray temperatures [i.e., NSHIP (“near-star-high-ion-problem”) introduced by WC07], and the overall radially-decreasing  $T_X$  distribution observed in OB supergiants as deduced by WC07. By using a mechanism suggested by CP84, self-contained diamagnetic plasmoids produced near OB stellar surfaces can be rapidly accelerated to speeds in excess of the ambient wind terminal velocity within  $2 R_*$ . These high speeds can only occur in the CP84 theory when the ejected plasmoids are initially magnetically dominated (i.e.,  $\beta_{po} \ll 1$ ). The acceleration is most strongly dependent on the plasmoid initial Alfvén speed ( $V_{Apo}$ ). Since our model fits demonstrate that a specific limit of  $V_{Apo} \leq 0.6V_{\infty}$  provides a physical explanation of the observed radially-dependent  $T_X$  upper bound for all normal OB stars, it seems that we have found a new upper limit to the initial plasmoid Alfvén speed for these stars. In addition, our derived  $\beta_{eo}$  and  $S$  parameters provide limits on the initial external plasma conditions. Our results demonstrate that *Chandra* observations have the potential to provide interesting information on the plasmoids and external plasma properties, and provide magnetic field constraints which are particularly relevant for those OB stars for which Zeeman measurements are not yet possible. Given the successful aspects and predictions of this plasmoid ejection model, further observations and detailed dynamical studies of magnetic propulsion mechanisms are clearly warranted.

We thank Vladimir Mirnov and Nicholas Murphy for helpful conversations. This work was supported in part by awards GO2-3027A and AR8-9003A issued by the *Chandra* X-ray Observatory Center, and the NSF Center for Magnetic Self-Organization in Laboratory and Astrophysical Plasmas. *Chandra* is operated by the Smithsonian Astrophysical Observatory under NASA contract NAS8-03060.

#### REFERENCES

- Abbott, D. C. 1982, *ApJ*, 259, 282  
 Bouret, J. -C., Donati, J. -F., Martins, F., Escolano, C., Marcolino, W., Lanz, T., & Howarth, I. D. 2008, *MNRAS*, 389, 75  
 Cargill, P. J., & Pneuman, G. W. 1984, *ApJ*, 276, 369 (CP84)  
 Cassinelli, J. P., Ignace, R., Waldron, W. L., Cho, J., Murphy, N. A., & Lazarian, A., 2008, *ApJ*, 683, 1052 (CAS08)  
 Cassinelli, J. P., & Swank, J. H. 1983, *ApJ*, 271, 681  
 Charbonneau, P., & MacGregor, K. B. 2001, *ApJ*, 559, 1094  
 Donati, J. -F., Babel, J., Harries, T. J., Howarth, I. D., Petit, P., & Semel, M. 2002, *MNRAS*, 333, 55  
 Donati, J. -F., Howarth, I. D., Bouret, J. -C., Petit, P., Catala, C., & Landstreet, J. 2006a, *MNRAS*, 365, 6  
 Donati, J. -F., Wade, G. A., Babel, J., Henrichs, H. F., de Jong, J. A., & Harries, T. J. 2001, *MNRAS*, 326, 1265  
 Donati, J. -F., et al. 2006b, *MNRAS*, 370, 629  
 Feldmeier, A. 1995, *A&A*, 299, 523  
 Ferrario, L., & Wickramasinghe, D. 2006, *MNRAS*, 367, 1323  
 Ferrario, L., & Wickramasinghe, D. 2005, *MNRAS*, 356, 615  
 Howk, J. C., Cassinelli, J. P., Bjorkman, J. E., & Lamers, H. J. G. L. M. 2000, *ApJ*, 534, 348  
 Lamers, H. J. G. L. M., & Cassinelli, J. P. 1999, *Introduction to Stellar Winds* (Cambridge: Cambridge Univ. Press)  
 MacGregor, K. B., & Cassinelli, J. P. 2003, *ApJ*, 586, 480  
 Maeder, A. 1980, *A&A*, 90, 311  
 Maeder, A. Georgy, C. & Meynet, G. 2008, *A&A*, 479, 37  
 Mullan, D. J., & MacDonald, J. 2005, *MNRAS*, 356, 1139  
 Neiner, C., Geers, V. C., Henrichs, H. F., Floquet, M., Fremat, Y., Hubert, A. -M., Preuss, O. & Wiersma, K. 2003, *A&A*, 406, 1019  
 Parker, E. N. 1957, *ApJS*, 3, 51  
 Petit, V., Wade, G. A., Drissen, L., Montmerle, T., & Alecian, E. 2008, *MNRAS*, 387, 23  
 Pneuman, G. W. 1983, *ApJ*, 265, 468  
 Schluter, A. 1957, in *IAU Symposium 4, Radio Astronomy*, ed., H. C. van de Hulst, (Cambridge: Cambridge University Press), p. 356

Waldron, W. L., & Cassinelli, J. P. 2001, ApJ, 548, L45  
Waldron, W. L., & Cassinelli, J. P. 2007, ApJ, 668, 456 (WC07)

Waldron, W. L., & Cassinelli, J. P. 2008, ApJ, 680, 1595 (WC08)  
Zwaan, C. 1985, Sol. Phys., 100, 397